PROCEEDINGS OF THE ROYAL SOCIETY A MATHEMATICAL, PHYSICAL & ENGINEERING SCIENCES

Revisiting the rocking block: closed-form solutions and similarity laws

Elias G. Dimitrakopoulos and Matthew J. DeJong

Proc. R. Soc. A 2012 **468**, 2294-2318 first published online 4 April 2012
doi: 10.1098/rspa.2012.0026

PROCEEDINGS OF THE ROYAL SOCIETY A

Proc. R. Soc. A (2012) **468**, 2294–2318
doi:10.1098/rspa.2012.0026
Published online 4 April 2012

Revisiting the rocking block: closed-form solutions and similarity laws

By Elias G. Dimitrakopoulos[1,*] and Matthew J. DeJong[2]

[1]*Department of Civil and Environmental Engineering, The Hong Kong University of Science and Technology, Kowloon, Clear Water Bay, Hong Kong*
[2]*Department of Engineering, University of Cambridge, Trumpington Street, Cambridge CB2 1PZ, UK*

In this paper, the dynamic response of the rocking block subjected to base excitation is revisited. The goal is to offer new closed-form solutions and original similarity laws that shed light on the fundamental aspects of the rocking block. The focus is on the transient dynamics of the rocking block under finite-duration excitations. An alternative way to describe the response of the rocking block, informative of the behaviour of rocking structures under excitations of different intensity, is offered. In the process, limitations of standard dimensional analysis, related to the orientations of the involved physical quantities, are revealed. The proposed dimensionless and orientationless groups condense the response and offer a lucid depiction of the rocking phenomenon. When expressed in the appropriate dimensionless–orientationless groups, the rocking response becomes perfectly self-similar for slender blocks (within the small rotations range) and practically self-similar for non-slender blocks (larger rotations). Using this formulation, the nonlinear and non-smooth rocking response to pulse-type ground motion can be directly determined, and need only be scaled by the intensity and frequency of the excitation.

Keywords: closed-form solutions; rocking; self-similarity; earthquake engineering; orientational analysis

1. Introduction

Rocking motion is increasingly being used to isolate structures from large stresses induced by earthquakes. These applications, in addition to intriguing non-smooth dynamic characteristics, have motivated a proliferation of literature on rocking structures (see Dimitrakopoulos & DeJong in press, and references therein). In this context, this paper offers an original, physically consistent description of the rocking block that elucidates the physical mechanism behind the dynamics of rocking structures under simple pulse excitations.

*Author for correspondence (ilias@ust.hk).

Electronic supplementary material is available at http://dx.doi.org/10.1098/rspa.2012.0026 or via http://rspa.royalsocietypublishing.org.

Received 18 January 2012
Accepted 6 March 2012

A major challenge of nonlinear structural dynamics is no longer the response analysis of a specific structural configuration, but rather the generic prediction of behaviour for a wide class of configurations. In the field of earthquake engineering, this challenge is exemplified by the definition of response spectra for nonlinear systems. To address this challenge, Makris & Black (2004) and Makris & Psychogios (2006) implemented formal dimensional analysis and showed that the response of yielding structures under pulse-type excitations is self-similar. Dimitrakopoulos *et al.* (2009*a*) extended the same approach to excitations without distinct pulses. The property of self-similarity has also been exploited for elastic or inelastic structures with pounding (Dimitrakopoulos *et al.* 2009*b*, 2010). Self-similarity is a symmetry/invariance with respect to a scale transformation of unique importance when ordering nonlinear phenomena (Sedov 1992; Barenblatt 1996). In structural dynamics (and earthquake engineering), self-similarity has the immediate consequence that response spectra become indifferent to the intensity and the frequency content of the excitation, even if the structural response is nonlinear and/or non-smooth.

The rocking response of a rigid block has been studied, in various scientific fields, for over a century (Augusti & Sinopoli 1992). The significant amount of analytical research focused on the steady-state response under harmonic loading (Hogan 1990) probably stems from the concept that a constant frequency excitation can cause resonance. However, constant frequency rocking resonance is impossible because the 'effective' frequency changes with rocking amplitude (DeJong *et al.* 2008). Furthermore, harmonic ground motions that could cause rocking resonance would have to have a precise time-varying frequency, and are thus extremely unlikely (DeJong 2012). Thus, from an earthquake engineering perspective, the transient rocking response to a finite-duration base excitation is of primary importance, rather than the steady-state response to harmonic loading (Zhang & Makris 2001).

This study comprises two parts. First, building on the work of Anooshehpoor *et al.* (1999) and Zhang & Makris (2001), among others, the overturning of the rocking block under a simple trigonometric pulse is considered and original closed-form solutions are presented. Second, the closed-form solutions clarify limitations of standard dimensional analysis (Barenblatt 1996), which does not incorporate the orientations of the involved physical quantities. However, the adoption of orientational analysis (Siano 1985) to supplement dimensional analysis enables identification of the self-similar rocking response.

2. Problem statement

During rocking of a single rigid block, continuous impact-free motion is interrupted by impacts at the pivot points. Hence, rocking is by definition a problem of non-smooth dynamics (Brogliato 1999; Glocker 2001). A complete description of a non-smooth dynamics problem requires, apart from the equations of motion (EOM), an appropriate treatment of impact. In particular, the problem of a rigid block rocking under a base excitation (figure 1) can be stated as follows:

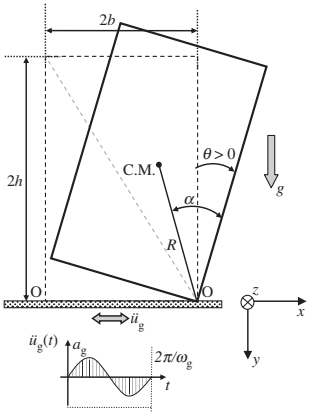

Figure 1. Geometry of the rigid rocking block under a pulse-type horizontal ground excitation.

(*a*) *Equations of motion*

Moment equilibrium around the rocking pivot point gives

$$\left.\begin{aligned} I_0\ddot{\theta} + mgR\sin(\alpha-\theta) &= -m\ddot{u}_g R\cos(\alpha-\theta), \quad \theta>0 \\ I_0\ddot{\theta} + mgR\sin(-\alpha-\theta) &= -m\ddot{u}_g R\cos(-\alpha-\theta), \quad \theta<0, \end{aligned}\right\} \tag{2.1}$$

where I_0 is the moment of inertia with respect to the pivot point, m is the mass of the block, g is the gravity acceleration, R is the half-diagonal (figure 1), α is the angle of slenderness, $\ddot{u}_g$ is the horizontal ground acceleration and θ is the response rotation. By geometry $\tan\alpha = b/h$, where $2b$ and $2h$ are the width and height of the block, respectively. Rocking initiates when $\ddot{u}_g \geq a_{g,\min} = g\tan\alpha$. Dividing equation (2.1) by I_0 yields

$$\frac{\ddot{\theta}}{p^2} = -\sin[\alpha\,\mathrm{sgn}(\theta)-\theta] - \frac{\ddot{u}_g}{g}\cos[\alpha\,\mathrm{sgn}(\theta)-\theta], \tag{2.2}$$

where $p=\sqrt{3g/4R}$ is the *frequency parameter* of the (rectangular) rocking block and $\mathrm{sgn}(\theta)$ is the standard sign function with: $\mathrm{sgn}(\theta=0)=0$, $\mathrm{sgn}(\theta<0)=-1$ and $\mathrm{sgn}(\theta>0)=1$. Equation (2.2) is a set of nonlinear ordinary differential equations that depend on the sign of the response rotation θ.

(*b*) *Treatment of impact*

Impact takes place when the rotation changes sign at $\theta=0$. There are several ways to treat impact (see Augusti & Sinopoli 1992; Prieto *et al.* 2004; Yilmaz *et al.* 2009 and references therein). In most cases, impact is described by a coefficient of restitution that relates the post-impact (angular) velocity $\dot{\theta}^+$ to the pre-impact velocity $\dot{\theta}^-$

$$\dot{\theta}^+ = \eta\dot{\theta}^-. \tag{2.3}$$

One way to estimate the coefficient of restitution is by equating the moment of momentum with respect to the forthcoming pivot point, just before and just after impact (Housner 1963).

The resulting coefficient of restitution for a rigid rectangular block (figure 1) is (Housner 1963)

$$\eta = 1 - \frac{3}{2}\sin^2\alpha. \tag{2.4}$$

However, for equation (2.4) to be valid, it is implicitly assumed that the block is slender enough, and the coefficient of friction high enough, to prevent other impact behaviours such as bouncing or sliding (Contento & Di Egidio 2009). In reality, it is clear that the coefficient of restitution is not a function of the geometry solely (see Prieto *et al.* 2004; ElGawady *et al.* 2010 and references therein), and hence equation (2.4) should be considered as a theoretical approximation of the coefficient of restitution needed to sustain pure rocking motion. For this reason, the coefficient of restitution is treated, in this study, as an independent parameter in the formulation of the rocking problem, as in Hogan (1989). Later in this paper, the influence of the coefficient of restitution on the response is analysed further.

3. Overturning of the rocking block: closed-form solutions

The overturning of a slender block under trigonometric pulses has been investigated in several studies, but the derivations herein primarily build on the work of Anooshehpoor *et al.* (1999) and Zhang & Makris (2001). In particular, the aim of this section is to derive closed-form solutions that completely describe the overturning of the rocking block under sine pulse excitations. In effect, this requires solving the transcendental equation that yields the time of impact.

For slender blocks (small α), the nonlinear EOM equation (2.2) can be linearized as

$$\ddot{\theta} - p^2\theta + p^2\alpha\,\mathrm{sgn}(\theta) = -p^2\frac{\ddot{u}_g}{g}. \tag{3.1}$$

Equation (3.1) is useful because simple mathematical excitations allow a closed-form analytical solution for the equation of motion (Housner 1963). Under a simple trigonometric excitation

$$\ddot{\theta} - p^2\theta + p^2\alpha\,\mathrm{sgn}(\theta) = \begin{cases} -p^2\dfrac{a_g}{g}\sin(\omega_g t + \psi), & \text{for } t \le T_{ex} \\ 0, & \text{for } t > T_{ex}, \end{cases} \tag{3.2}$$

where a_g and $\omega_g = 2\pi/\mathrm{T}_p$ (figure 1) are the acceleration amplitude and the angular frequency of the pulse, α is the angle of slenderness and p is the frequency parameter. The time instant when the excitation expires is $T_{ex} = (2\pi - \psi)/\omega_g$, and ψ is the phase when rocking initiates. Note that the phase angle defines $t = 0$ as the instant that rocking initiates, not the instant that the pulse initiates. For a sine pulse excitation

$$\sin\psi = \frac{\alpha g}{a_g} \doteq \frac{1}{\alpha}, \quad \cos\psi = \cos\left(\arcsin\left(\frac{1}{a}\right)\right) = \sqrt{1 - \left(\frac{1}{a}\right)^2}, \quad \psi = \arcsin\left(\frac{1}{a}\right). \tag{3.3}$$

The solution of equation (3.2) for the forced rocking stage $t \le T_{ex}$ yields

$$\left.\begin{aligned} \frac{\theta(\tau)}{\alpha} &= \operatorname{sgn}(\theta) + \frac{a}{\omega^2+1}\sin(\omega\tau+\psi) + \frac{A}{\alpha}\mathrm{e}^{-\tau} + \frac{B}{\alpha}\mathrm{e}^{\tau} \\ \text{and} \quad \frac{\dot\theta(\tau)}{p\alpha} &= \frac{B}{\alpha}\mathrm{e}^{\tau} - \frac{A}{\alpha}\mathrm{e}^{-\tau} + \frac{a\omega}{\omega^2+1}\cos(\omega\tau+\psi). \end{aligned}\right\} \tag{3.4}$$

The pertinent solutions for the free rocking stage $t > T_{ex}$ phase are

$$\left.\begin{aligned} \frac{\theta(\tau)}{\alpha} &= \operatorname{sgn}(\theta) + \frac{A}{\alpha}\mathrm{e}^{-\tau} + \frac{B}{\alpha}\mathrm{e}^{\tau} \\ \text{and} \quad \frac{\dot\theta(\tau)}{p\alpha} &= \frac{B}{\alpha}\mathrm{e}^{\tau} - \frac{A}{\alpha}\mathrm{e}^{-\tau}, \end{aligned}\right\} \tag{3.5}$$

where the following dimensionless groups are used

$$\omega \doteq \frac{\omega_g}{p}, \quad \tau \doteq pt, \quad \text{and} \quad a \doteq \frac{a_g}{g\alpha}. \tag{3.6}$$

The overturning problem of the rocking block can be broken down (figure 2) to the following cases (Anooshehpoor *et al.* 1999): overturning without impact (case 2) or overturning with impact taking place before (case 1.1) or after (case 1.2) the end of the excitation. The constants A and B depend on the initial conditions of each response stage (figure 2) and the time instant the stage initiates.

For zero initial conditions $\theta(\tau=0)=0$, $\dot\theta(\tau=0)=0$ (and for a sine excitation) the constants $A=A_0$ and $B=B_0$ simplify to

$$A_0 = \frac{\alpha}{2}\left(\frac{\omega^2+\omega\sqrt{a^2-1}}{\omega^2+1}\right), \quad \text{and} \quad B_0 = \frac{\alpha}{2}\left(\frac{\omega^2-\omega\sqrt{a^2-1}}{\omega^2+1}\right). \tag{3.7}$$

Following figure 2, each possible response sequence will be analysed separately, starting from the simplest case (case 2) and moving on to the most complex one (case 1.1). In all cases (of figure 2), it is assumed that under the minimum amplitude ground acceleration which will cause overturning for a given pulse duration, overturning takes place during the free rocking stage when the velocity tends to a minimum for large time t (Zhang & Makris 2001):

$$\ddot\theta(t_\infty) = 0 \Rightarrow B = 0. \tag{3.8}$$

Note that $B=0$ defines the pertinent unstable manifold of the rocking block (Hogan 1989).

The following notation will be used in the sections that follow

$$\begin{aligned} A_0^* &= 2\frac{A_0}{\alpha} = \frac{\omega^2+\omega\sqrt{a^2-1}}{\omega^2+1}, \quad B_0^* = 2\frac{B_0}{\alpha} = \frac{\omega^2-\omega\sqrt{a^2-1}}{\omega^2+1}, \quad C_0^* = \frac{2a}{\omega^2+1}, \\ D_0^* &= \left(A_0^* - \frac{\omega}{2}C_0^*\mathrm{e}^{pT_{ex}}\right)\left(B_0^* + \frac{\omega}{2}C_0^*\mathrm{e}^{-pT_{ex}}\right) \\ &= \frac{\omega}{\omega^2+1}\left(\omega^2 - 2a^2 + 1 + \left(\sqrt{a^2-1}+\omega\right)a\mathrm{e}^{-pT_{ex}} + \left(\sqrt{a^2-1}-\omega\right)a\mathrm{e}^{pT_{ex}}\right). \end{aligned} \tag{3.9}$$

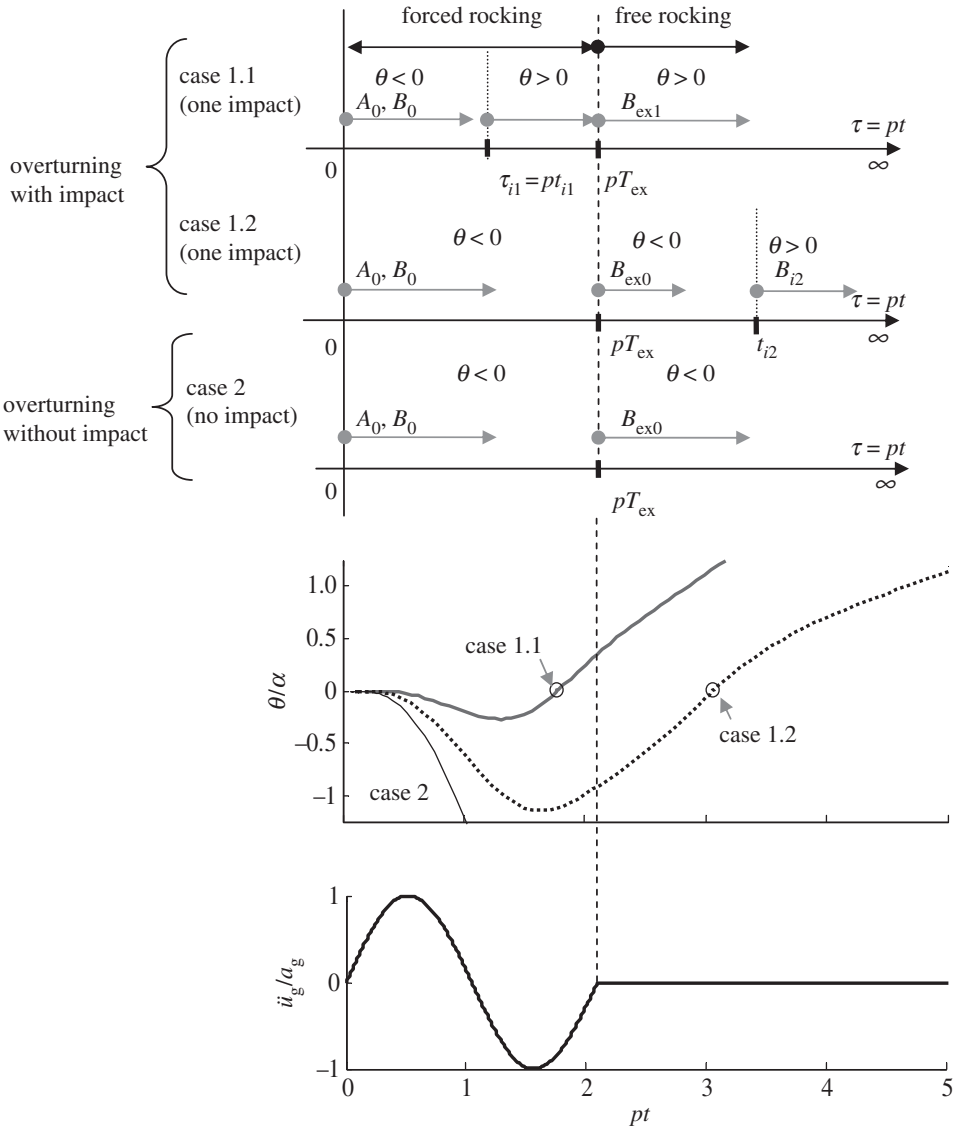

Figure 2. Top: possible response sequences of a rocking block excited by a sine pulse, including initial conditions (A, B) and the sign of rocking rotation θ for each response stage. Bottom: sample time-history response for each case.

(*a*) *Overturning case 2*

In the case of overturning without impact, the overturning condition becomes

$$\left.\begin{aligned} B_{\mathrm{ex0}} = 0 \Rightarrow \frac{\theta_{\mathrm{ex0}}}{\alpha} + \frac{\dot{\theta}_{\mathrm{ex0}}}{p\alpha} + 1 = 0 \Rightarrow B_0^* \mathrm{e}^{pT_{\mathrm{ex}}} + \frac{\omega}{2} C_0^* = 0 \Leftrightarrow \\ \text{and} \qquad \omega = \sqrt{a^2 - 1} - a\mathrm{e}^{-pT_{\mathrm{ex}}} \Leftrightarrow \omega = \sqrt{a^2 - 1} - a\mathrm{e}^{-\frac{2\pi - \arcsin(1/a)}{\omega}}. \end{aligned}\right\} \tag{3.10}$$

As expected, the overturning condition equation (3.10) does not depend on the coefficient of restitution η, but only on the dimensionless groups a and ω. The difference between equation (3.10) and the pertinent equations of Anooshehpoor *et al.* (1999) and Zhang & Makris (2001) is that exponential functions are used here instead of hyperbolic trigonometric functions. The choice of exponential functions might be trivial in the case of equation (3.10) but turns out to be important in cases 1.1 and 1.2, where a solution to transcendental equations is sought.

(*b*) *Overturning case 1.2*

At the end of the excitation and assuming no impact has taken place (figure 2), the rotation and the velocity are

$$\frac{\theta_{\mathrm{ex0}}}{\alpha}=\frac{1}{2}A_0^*\mathrm{e}^{-pT_{\mathrm{ex}}}+\frac{1}{2}B_0^*\mathrm{e}^{pT_{\mathrm{ex}}}-1,\quad \frac{\dot{\theta}_{\mathrm{ex0}}}{p\alpha}=\frac{1}{2}(B_0^*\mathrm{e}^{pT_{\mathrm{ex}}}-A_0^*\mathrm{e}^{-pT_{\mathrm{ex}}}+C_0^*\omega). \tag{3.11}$$

The time instant impact occurs $\tau_{i2}=pt_{i2}$ (within case 1.2) can be determined from

$$\theta(\tau_{i2})=0\Rightarrow\left(A_0^*-\frac{\omega}{2}C_0^*\mathrm{e}^{pT_{\mathrm{ex}}}\right)\mathrm{e}^{-\tau_{i2}}+\left(B_0^*+\frac{\omega}{2}C_0^*\mathrm{e}^{-pT_{\mathrm{ex}}}\right)\mathrm{e}^{\tau_{i2}}-2=0. \tag{3.12}$$

Extending previous works (Anooshehpoor *et al.* 1999; Zhang & Makris 2001), the time of impact can be calculated directly and inserted in the pertinent overturning condition (equation (3.18)). The transcendental equation (3.12) can be solved exactly using an appropriate change of variables (see appendix A). The negative solution of equation (3.12) lacks physical meaning. The time of impact is given by the positive solution

$$\tau_{i2}=\ln\left(\frac{1+\sqrt{1-D_0^*}}{B_0^*+\frac{\omega}{2}C_0^*\mathrm{e}^{-pT_{\mathrm{ex}}}}\right). \tag{3.13}$$

The pertinent pre-impact velocity $\dot{\theta}_{i2}$ is given, in dimensionless terms, by

$$2\frac{\dot{\theta}_{i2}}{p\alpha}=\left(B_0^*+\frac{\omega}{2}C_0^*\mathrm{e}^{-pT_{\mathrm{ex}}}\right)\mathrm{e}^{\tau_{i2}}-\left(A_0^*-\frac{\omega}{2}C_0^*\mathrm{e}^{pT_{\mathrm{ex}}}\right)\mathrm{e}^{-\tau_{i2}}. \tag{3.14}$$

After substitution of the time of impact

$$\frac{\dot{\theta}_{i2}}{p\alpha}=\sqrt{1-D_0^*}. \tag{3.15}$$

Finally, after impact it is assumed that the block for sufficiently large time, overturns. Thus, the overturning condition simplifies to (figure 2)

$$B_{i2}=0, \tag{3.16}$$

or

$$\eta\frac{\dot{\theta}_{i2}}{p\alpha}=1\Rightarrow\left(B_0^*+\frac{\omega}{2}C_0^*\mathrm{e}^{-pT_{\mathrm{ex}}}\right)\mathrm{e}^{\tau_{i2}}-\left(A_0^*-\frac{\omega}{2}C_0^*\mathrm{e}^{pT_{\mathrm{ex}}}\right)\mathrm{e}^{-\tau_{i2}}=\frac{2}{\eta}, \tag{3.17}$$

which, after some algebra, yields

$$1-\left[A_0^*B_0^*-\left(\frac{\omega}{2}C_0^*\right)^2+\frac{\omega}{2}C_0^*\left(A_0^*\mathrm{e}^{-pT_{\mathrm{ex}}}-B_0^*\mathrm{e}^{pT_{\mathrm{ex}}}\right)\right]=\frac{1}{\eta^2}. \tag{3.18}$$

Equation (3.18) is the exact expression for the overturning envelope when impact takes place after the excitation has ceased (case 1.2 of figure 2).

(*c*) *Overturning case 1.1*

When impact takes place before the end of the excitation (figure 2), the associated overturning condition is

$$B_{\mathrm{ex1}}=0, \tag{3.19}$$

which yields

$$2\eta\frac{\dot{\theta}_{i1}}{p\alpha}+C_0^*[\omega\mathrm{e}^{-pT_{\mathrm{ex}}}\,\mathrm{e}^{\tau_{i1}}-\omega\cos(\omega\tau_{i1}+\psi)-\sin(\omega\tau_{i1}+\psi)]=2, \tag{3.20}$$

where $\dot{\theta}_{i1}$ is the unknown pre-impact velocity and τ_{i1} is the unknown pertinent time instant. The (dimensionless) time of impact $\tau_{i1}=pt_{i1}$ can be determined by solving numerically the transcendental equation

$$\theta(\tau_{i1})=0\Rightarrow A_0^*\mathrm{e}^{-\tau_{i1}}+B_0^*\mathrm{e}^{\tau_{i1}}+C_0^*\sin(\omega\tau_{i1}+\psi)-2=0. \tag{3.21}$$

By substituting τ_{i1} into equation (3.22), the pre-impact velocity can be calculated

$$2\frac{\dot{\theta}(\tau_i)}{p\alpha}=B_0^*\mathrm{e}^{\tau_i}-A_0^*\mathrm{e}^{-\tau_i}+C_0^*\omega\cos(\omega\tau_i+\psi). \tag{3.22}$$

In figure 3, the 'numerical' overturning curves for case 1.1 are plotted using equations (3.20) and (3.21).

Alternatively, in order to capture the overturning according to case 1.1 with a closed-form formula, a solution to the transcendental equation (3.21) is needed. The change of variables used in the previous case (case 1.2) cannot be used directly to solve equation (3.21) because the non-exponential term is not constant. Furthermore, other dependable approaches (Mylonakis & Voyagaki 2006) for solving analytically similar transcendental equations are not applicable in this case.

Instead, a novel approach for approximating analytically the solution of the transcendental equation (3.21), i.e. the dimensionless impact time $\hat{\tau}_{i1}$ (equation (3.21)), is proposed herein. The basic assumption, verified by numerical analyses, is that the time the block takes to return to its rest position (impact) after the rocking initiates is approximately $1/p$, which means that

$$t_{i1}^0\simeq\frac{1}{p}\Rightarrow\tau_{i1}^0=pt_{i1}^0=1. \tag{3.23}$$

Hence, in the following, the non-constant trigonometric function $\sin(\omega\tau+\psi)$ is approximated locally (around $\tau_{i1}^0=1$) with an ad hoc function $\kappa\mathrm{e}^{-\tau}+\lambda\mathrm{e}^{\tau}$ of the two exponential functions $\mathrm{e}^{-\tau}$, e^{τ}. For this purpose, the sine function is first

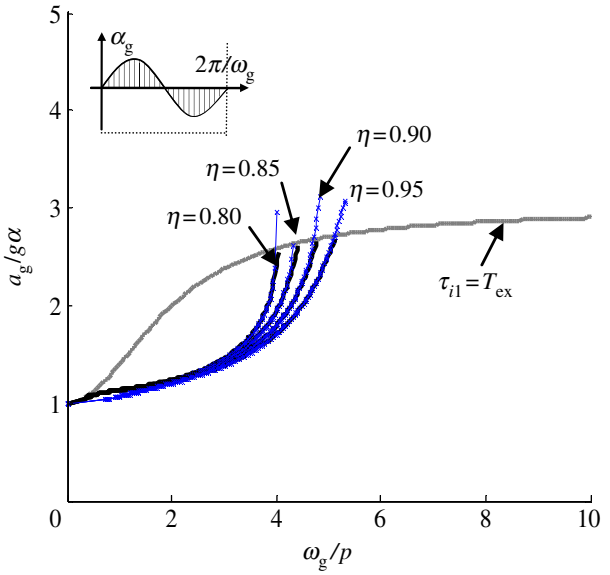

Figure 3. Comparison of numerical (black line) (equations (3.20) and (3.28)) and semi-analytical (blue line) (equation (3.30)) results for the curve that delineates overturning for case 1.1. (Online version in colour.)

expanded in series at $\tau = 1$, keeping up to second-order terms

$$\sin(\omega\tau + \psi) \simeq \sin(\omega + \psi) + \omega\cos(\omega + \psi)(\tau - 1) - \frac{\omega^2}{2}\sin(\omega + \psi)(\tau - 1)^2 \quad (3.24)$$

The ad hoc function $\kappa e^{-\tau} + \lambda e^{\tau}$ is also expanded in series at $\tau = 1$ keeping up to second-order terms

$$\kappa e^{-\tau} + \lambda e^{\tau} \simeq \left(\frac{\kappa}{e} + \lambda e\right) + \left(\lambda e - \frac{\kappa}{e}\right)(\tau - 1) + \left(\frac{\kappa}{2e} + \frac{\lambda e}{2}\right)(\tau - 1)^2. \quad (3.25)$$

Coefficients κ and λ are determined by equating the two polynomial approximations

$$\kappa = -\frac{e\omega}{2}[\cos(\omega + \psi) + \omega\sin(\omega + \psi)], \quad \lambda = \frac{\omega}{2e}[\cos(\omega + \psi) - \omega\sin(\omega + \psi)]. \quad (3.26)$$

Thus, the trigonometric function $\sin(\omega\tau + \psi)$ can be approximated, at around $\tau_{i1}^0 = 1$, as

$$\sin(\omega\tau + \psi) = (\omega^2 + 1)\sin(\omega + \psi) + \kappa e^{-\tau} + \lambda e^{\tau}. \quad (3.27)$$

Appendix B of the electronic supplementary material (figure S1) illustrates the accuracy of the proposed approximation for different $\omega = \omega_g/p$ ratios. The approximation is satisfactory (around $\tau = 1$) for intermediate values of $\omega \approx 5$ and excellent for small values of $\omega < 2$. For $\omega > 5$, the block does not overturn according to case 1.1 and hence there is no need to consider higher values.

Substituting equation (3.27) into equation (3.21) yields

$$\theta(t_{i1}) = 0 \Rightarrow (A_0^* + C_0^*\kappa)\mathrm{e}^{-\tau} + (B_0^* + C_0^*\lambda)\mathrm{e}^{\tau} + 2[a\sin(\omega+\psi) - 1] = 0 \tag{3.28}$$

which can be solved exactly (see appendix A). Keeping only the positive solution returns

$$\hat{\tau}_{i1} = \ln\left(\frac{1 - a\,\sin(\omega+\psi) + \sqrt{[a\,\sin(\omega+\psi) - 1]^2 - (A_0^* + C_0^*\kappa)(B_0^* + C_0^*\lambda)}}{B_0^* + C_0^*\lambda}\right), \tag{3.29}$$

where the 'hat' denotes approximation. Using equation (3.29), the overturning condition for case 1.1 can be simplified further to

$$\begin{aligned}&\eta[B_0^*\mathrm{e}^{\hat{\tau}_{i1}} - A_0^*\mathrm{e}^{-\hat{\tau}_{i1}} + C_0^*\omega\cos(\omega\hat{\tau}_{i1}+\psi)]\\ &\quad + C_0^*[\omega e^{-pT_{\mathrm{ex}}}\mathrm{e}^{\hat{\tau}_{i1}} - \omega\cos(\omega\hat{\tau}_{i1}+\psi) - \sin(\omega\hat{\tau}_{i1}+\psi)] = 2.\end{aligned} \tag{3.30}$$

Figure 3 offers the comparison of these two approaches, the former of which is named 'numerical' (equations (3.20) and (3.21)) and the latter 'semi-analytical' (equation (3.30)). The minimum solution provided by equation (3.30) coincides with the pertinent solution of equations (3.20) and (3.21) verifying the accuracy of the approximation (equation (3.29)). This approximation (equation (3.29)) is an original contribution that simplifies further the description of the overturning behaviour of the rocking block.

(*d*) *Limit* $\tau_{\mathrm{i}} = pT_{\mathrm{ex}}$

The two cases: case 1.1 and case 1.2 are distinguished by the limit: $\tau_{i1} = \tau_{i2} = pT_{\mathrm{ex}}$ or equivalently: $t_{i1} = t_{i2} = T_{\mathrm{ex}}$. This limit is calculated by equating the time of impact (either from equation (3.12) or from equation (3.21)) with the time instant the excitation ends

$$1 + \sqrt{1 - A_0^*B_0^*} = B_0^*\mathrm{e}^{pT_{\mathrm{ex}}} \Rightarrow 1 + \omega^2 + \sqrt{1 + (a^2+1)\omega^2} = \left(\omega^2 - \omega\sqrt{a^2-1}\right)\mathrm{e}^{pT_{\mathrm{ex}}}. \tag{3.31}$$

Equation (3.31) is also offered by Anooshehpoor *et al.* (1999).

In summary, in the case of a sine pulse excitation, and under the assumptions aforementioned, the overturning of the rocking block can be captured completely on the control space (a, ω, η) with the four closed-form expressions: equations ((3.10), (3.18), (3.30)) (or equations (3.20) and (3.21) instead) and equation (3.31) as in figure 4.

The area of the control space enclosed by the two curves defined by equation (3.18) for case 1.1 and by equation (3.30) (or equivalently by equations (3.20) and (3.21)) for case 1.2 corresponds to overturning after one impact. The area above the curve defined by equation (3.10) corresponds to overturning without impact. The remaining area of the control space, the 'safe' area, is divided by the $\tau_{i1} = \tau_{i2} = pT_{\mathrm{ex}}$ curve into two regions: the region below the curve where the first impact occurs before the end of the excitation, and the region above the curve where the first impact occurs after the end of the excitation. This simplifies the rocking problem further, as will be illustrated later. The semi-analytical overturning plots (figure 4) are in excellent agreement with the pertinent numerical ones (Dimitrakopoulos & DeJong in press).

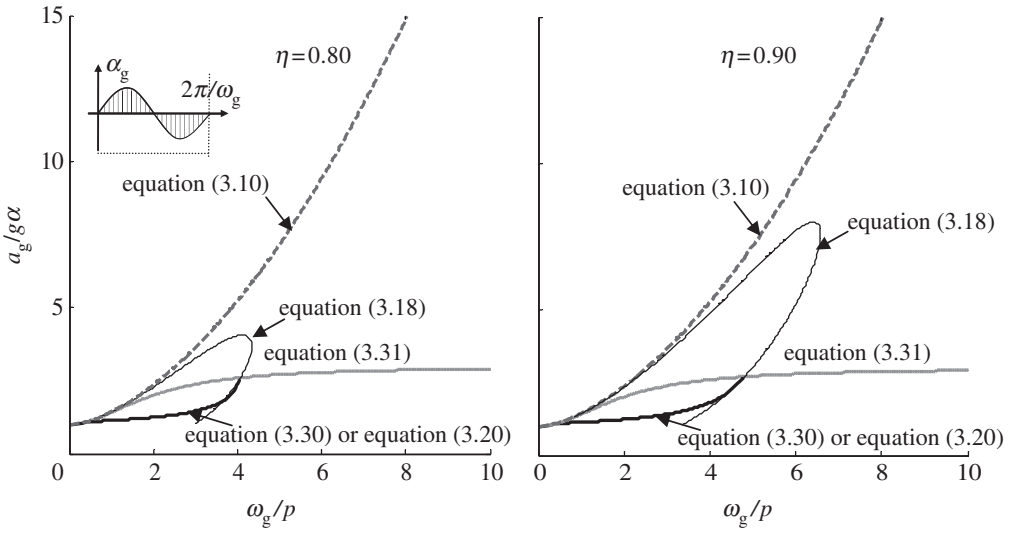

Figure 4. Overturning plots for different values of η calculated using the closed-form expressions in equations (3.10), (3.18), (3.30) (or equations (3.20) and (3.21) instead) and equation (3.31).

Thus, closed-form solutions that completely describe the overturning of the rocking block are provided. The procedure illustrated for a sine pulse excitation can be mimicked for other trigonometric pulses. For excitations with more loading cycles, more overturning sequences would arise and the analysis would lengthen rapidly.

4. Slender rocking block: similarity laws

While §3 dealt with the overturning of the rocking block, this section focuses on the rocking response of the block when it survives the motion. Hinging upon the analytical solutions presented in §3, the aim of this section is to offer a useful self-similar description of the rocking block and bring forward a shortcoming of standard dimensional analysis.

As a first approach, the rocking rotation can be normalized with respect to the slenderness of the block α (figure 1) as in equation (3.4). Following this approach, differentiation with respect to the dimensionless time $\tau = pt$ yields the dimensionless angular velocity $\dot{\theta}/p\alpha$, not just $\dot{\theta}/p$. While this formulation (equation (3.4)) clarifies the fundamental behaviour of rocking systems, a more direct scaling of the rocking response to the excitation intensity is sought. To this end, an alternative approach is to normalize the response with meaningful scales of the excitation rather than with characteristics of the block (e.g. slenderness α). Multiplying equation (3.5) with the dimensionless group $1/a = g\alpha/a_g$ yields

$$\left.\begin{aligned} \frac{g\theta(\tau)}{a_g} &= \frac{1}{a}\mathrm{sgn}(\theta) + \frac{1}{\omega^2+1}\sin(\omega\tau+\psi) + \frac{g}{a_g}A\mathrm{e}^{-\tau} + \frac{g}{a_g}B\mathrm{e}^{\tau} \\ \text{and} \qquad \frac{g\dot{\theta}(\tau)}{pa_g} &= \frac{g}{a_g}B\mathrm{e}^{\tau} - \frac{g}{a_g}A\mathrm{e}^{-\tau} + \frac{\omega}{\omega^2+1}\cos(\omega\tau+\psi). \end{aligned}\right\} \tag{4.1}$$

The proposed dimensionless groups (equation (4.1)) hinge upon the characteristics of a pulse-type excitation, a_g and $\omega_g = 2\pi/T_p$.

It is interesting to note, that neither the dimensionless groups of equation (3.4) nor the dimensionless groups of equation (4.1) can be derived from formal dimensional analysis. In particular, the maximum rotation θ_{max} of the rocking block can be written as a function of the general form

$$\theta_{max} = f\left(\alpha, p, \frac{a_g}{g}, \omega_g, \eta\right). \tag{4.2}$$

Equation (3.31) contains six characteristic variables that involve only one reference dimension, time $[T]$. According to Buckingham's 'Π' theorem (Buckingham 1914), the number of independent dimensionless Π-products is five

$$\theta_{max} = \phi\left(\omega, \frac{a_g}{g}, \alpha, \eta\right), \tag{4.3}$$

where the only dimensionless term arising from dimensional analysis is the ratio $\omega = \omega_g/p$. According to dimensional analysis, dimensionless quantities cannot be combined. Hence, formal dimensional analysis yields very little benefit for the rocking problem, because the already dimensionless groups of equation (4.3) cannot be combined to yield the dimensionless groups of equation (3.4) or equation (4.1).

However, if one distinguishes the notion of dimension to that of orientation (see Siano 1985; Araneda 1996), then the groups derived from Buckingham's theorem are dimensionless but are not orientationless. One can supplement dimensional analysis taking into account the orientations (Siano 1985) of the involved characteristic variables and demanding that the physical equations be both dimensionally *and orientationally* homogeneous. For instance, the maximum rocking rotation θ_{max} and the slenderness α are dimensionless but not orientationless, in contrast with the coefficient of restitution η which is both dimensionless and orientationless.

At this point, it is necessary to introduce multiplication rules for orientations. Let l_x, l_y and l_z denote the unit orientations along the x-, y- and z-axis, respectively, and let l_0 be the identity element (no orientation). The following rules apply (Siano 1985)

$$l_x \mathrel{\mathring{=}} l_x^{-1}, \quad l_x^2 \mathrel{\mathring{=}} l_0, \tag{4.4}$$

where $\mathring{=}$ denotes orientational equality. Similar rules hold for orientations y, z and the orientationless element l_0. In addition

$$l_x^{2n+1} \mathrel{\mathring{=}} l_x, \quad l_x^{2n} \mathrel{\mathring{=}} l_0, \tag{4.5}$$

for any integer n. The multiplication rules of the orientational symbols (l_x, l_y, l_z and l_0) are summarized in table 1.

Following the reasoning of orientational analysis, an angle θ in the x–y plane is l_z oriented. Siano (1985) demonstrated this point for a small angle θ : $\tan\theta = \sin\theta/\cos\theta \mathrel{\mathring{=}} l_z/l_0 \mathrel{\mathring{=}} lz$, because $\sin\theta \simeq \theta \mathrel{\mathring{=}} l_z$, and $\cos\theta \simeq l \mathrel{\mathring{=}} 1_0$. The orientation of trigonometric functions can also be derived by using the pertinent power

Table 1. Multiplication table of the unit orientations.

	l_0	l_x	l_y	l_z
l_0	l_0	l_x	l_y	l_z
l_x	l_x	l_0	l_z	l_y
l_y	l_y	l_z	l_0	l_x
l_z	l_z	l_y	l_x	l_0

expansion series, for example

$$\cos\theta = \underbrace{1}_{l_0} - \underbrace{\frac{\theta^2}{2!}}_{l_0} + \underbrace{\frac{\theta^4}{4!}}_{l_0} - \underbrace{\frac{\theta^6}{6!}}_{l_0} \cdots \Rightarrow \cos\theta \mathrel{\dot{=}} l_0. \tag{4.6}$$

Accordingly, the orientations of the characteristic variables of the rocking block problem can now be determined

$$\theta \mathrel{\dot{=}} l_z, \quad \omega = \frac{\omega_g}{p} \mathrel{\dot{=}} \frac{l_0}{l_0} \mathrel{\dot{=}} l_0, \quad \frac{a_g}{g} \mathrel{\dot{=}} \frac{l_x}{l_y} \mathrel{\dot{=}} l_z, \quad \alpha \mathrel{\dot{=}} l_z, \quad \eta \mathrel{\dot{=}} l_0. \tag{4.7}$$

Note that in figure 1, orientation z is perpendicular to the page. Furthermore, according to orientational analysis (Siano 1985), angular frequency is orientationless, hence the frequency parameter p is orientationless. Orientational homogeneity of equation (4.3) requires

$$\theta_{\max} = \phi\left(\omega, \frac{a_g}{a}, \alpha, \eta\right) \rightarrow l_z \mathrel{\dot{=}} l_0^{\varepsilon_1} l_z^{\varepsilon_2} l_z^{\varepsilon_3} l_0^{\varepsilon_4} \Rightarrow l_z \mathrel{\dot{=}} l_z^{\varepsilon_2+\varepsilon_3}, \tag{4.8}$$

which yields

$$\varepsilon_2 + \varepsilon_3 = \text{odd number}. \tag{4.9}$$

Orientational analysis, as proposed by Siano (1985), does not yield a definite value for the unknown exponents ε_2 and ε_3. Instead, it provides constraints (e.g. equation (4.9)) which can be useful in combination with physical reasoning or mathematical derivation. In our case, it can be used to confirm that the dimensionless–orientationless groups derived from analytical manipulations may indeed provide a self-similar response. Choosing $\varepsilon_2 = 1$ and $\varepsilon_3 = -2$, the dimensionless (and orientationless) groups of equation (3.4) are retrieved

$$\frac{\theta}{\alpha} = \phi\left(\frac{\omega_g}{p}, \frac{a_g}{\alpha g}, pt, \eta\right) = \phi(\omega, a, \tau, \eta). \tag{4.10}$$

Alternatively, choosing $\varepsilon_2 = -2$ and $\varepsilon_3 = 1$, the dimensionless (and orientationless) groups of equation (4.1) are found

$$\frac{\theta g}{a_g} = \phi\left(\frac{\omega_g}{p}, \frac{\alpha g}{a_g}, pt, \eta\right) = \phi\left(\omega, \frac{1}{a}, \tau, \eta\right). \tag{4.11}$$

The main advantage of the proposed dimensionless–orientationless approach is that it brings forward the property of self-similarity in the rocking response in a general method, for any excitation that can be described using amplitude a_g

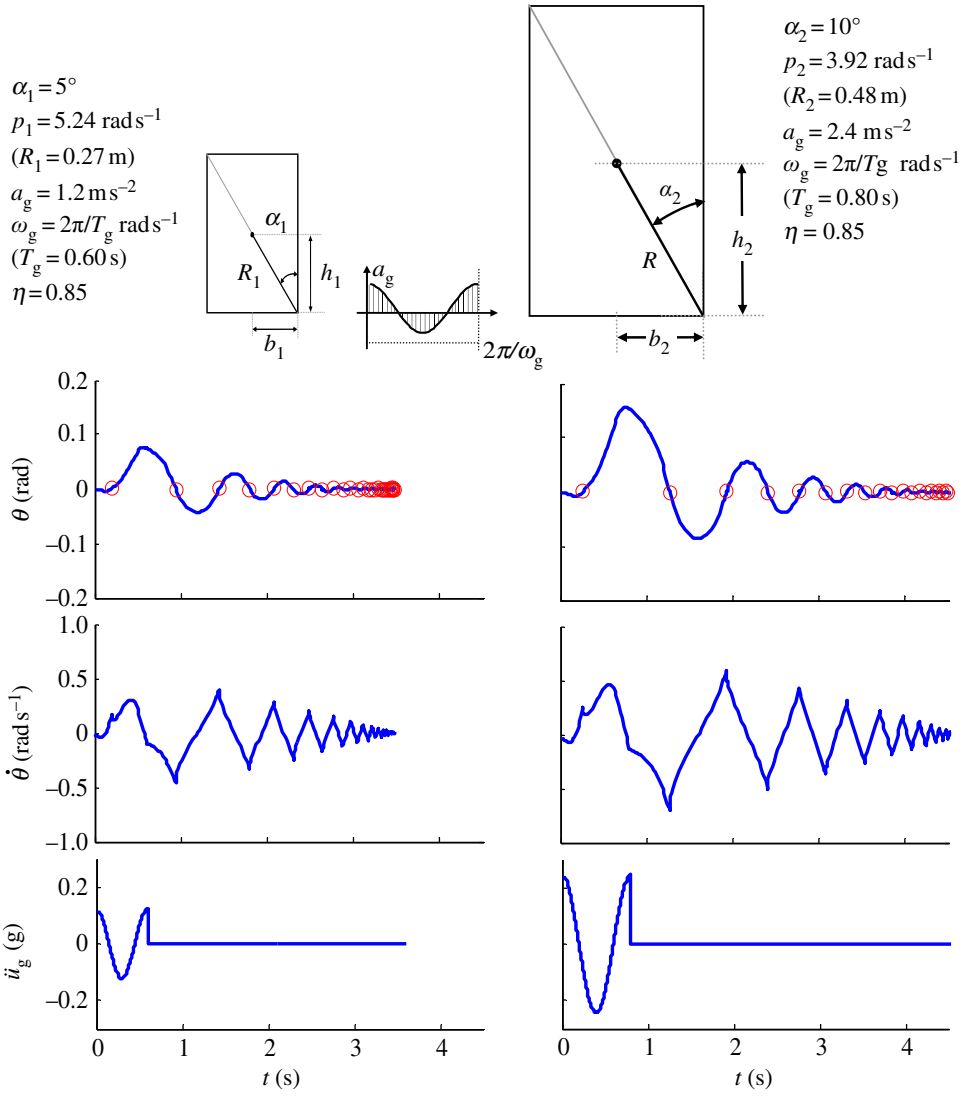

Figure 5. The response (equation (3.3)) of two rocking blocks of different shape and size. The dimensionless–orientationless terms that describe the behaviour are equal in both cases. (Online version in colour.)

and frequency ω_g, which is not achieved by the previous closed-form solutions. Figure 5 plots the response of two rigid blocks subjected to one-cosine acceleration pulses of different amplitude a_g and frequency $\omega_g = 2\pi/T_g$. The blocks differ in size (p) and shape (α). However, the associated dimensionless–orientationless groups, including the coefficient of restitution ($\eta = 0.85$), are equal in both cases. The response time histories are calculated numerically from the linearized EOM (equation (3.2)) and are presented in dimensional terms.

When the same response curves are plotted in the proposed dimensionless terms, they collapse to a single 'master' curve (figure 6). In other words, the analysis shows that the critical parameters for the rocking response of a rigid

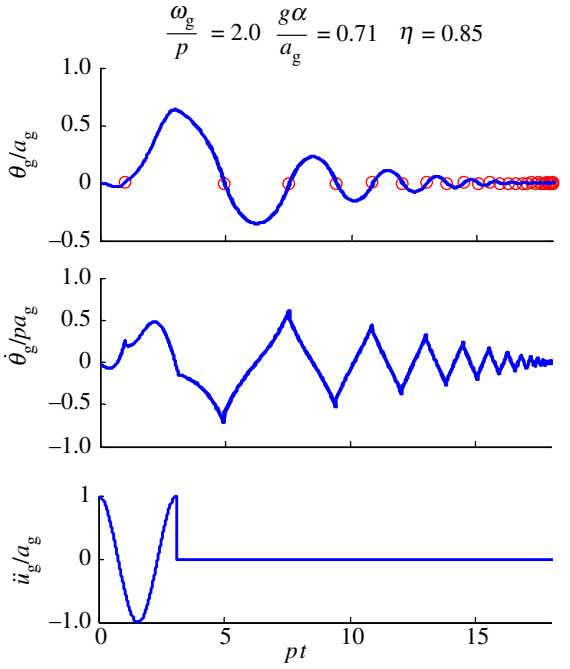

Figure 6. Self-similar response (small-angle approximation): when the response is presented in the proposed dimensionless–orientationless terms, the two cases of figure 5 collapse to a single curve. (Online version in colour.)

block, for a given coefficient of restitution η, are the dimensionless–orientationless slenderness $1/a = g\alpha/a_g$ and the frequency ratio $\omega = \omega_g/p$. These parameters alone are sufficient to define a unique response.

(*a*) *A scale law for the coefficient of restitution*

While dimensional and orientational analysis have significantly reduced the parameters involved, the dependence on the coefficient of restitution prevents the production of a single curve that defines overturning or maximum response. This section investigates the possibility of simplifying the dependence on the coefficient of restitution by deriving an appropriate scaling relation. Figure 7 presents numerical results (equation (3.3)) for the rocking rotation and angular velocity for fixed values of $\omega = \omega_g/p$ and $1/a = g\alpha/a_g$ but a varying coefficient of restitution η. As the coefficient of restitution decreases, the effective period becomes shorter and the maximum response (rotation and angular velocity) lower. This is a damping mechanism that is well documented (Priestley *et al.* 1978).

Similarly, figure 8 plots rocking spectra (solid lines), obtained from the integration of the linear equation of motion (equation (3.2)), in the proposed dimensionless–orientationless terms for coefficients of restitution ranging from $\eta = 0.80$ to 0.96 (intervals of 0.02). Both figures 7 and 8 indicate the possibility of a scale law to account for the varying coefficient of restitution. For the sine pulse excitation apart from the numerical results, figure 8 also shows (dashed lines) the results obtained from the subsequent analysis.

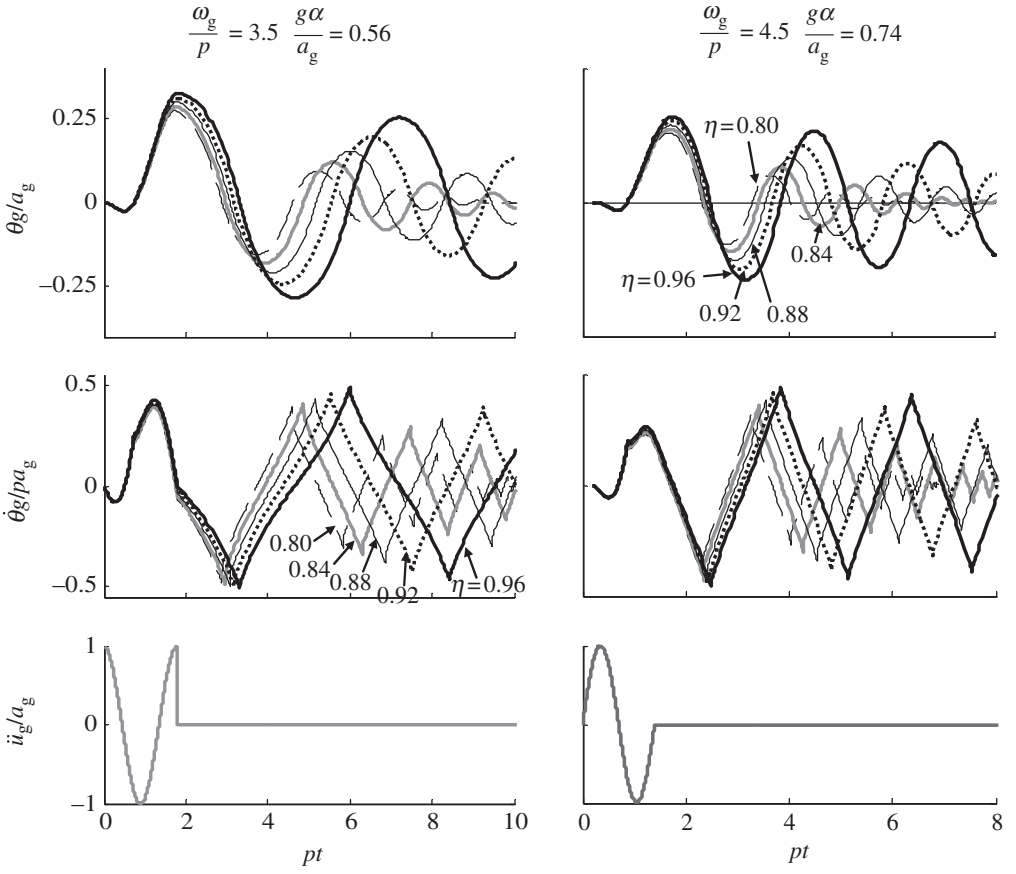

Figure 7. Time histories (equation (3.3)) for a different coefficient of restitution η (=0.80–0.96), but given ω_g/p and $\alpha g/a_g$ values. The varying coefficient of restitution results in a damping effect.

To investigate the possibility of a scale law, the closed-form solutions derived previously are employed. Recall that for the safe area of the control space (figure 4) above the curve $\tau_i = pT_{ex}$ (equation (3.31)), the first impact takes place after the end of the excitation (case 1.2) and the block survives the motion. The maximum rotation appears either during the excitation or after the first impact (which takes place after the end of the excitation). As $\omega = \omega_g/p$ becomes larger, the loading is more reminiscent to an impulse loading and thus the maximum rotation appears after the end of the excitation. Assuming this case dominates, conservation of energy (for small rotations) after the first impact can be used to determine the maximum rotation angle

$$\frac{1}{2}I(\eta\dot{\theta}_{i2})^2 = mgR[1-\cos(\alpha-\theta_m)] \Rightarrow \frac{\theta_m}{\alpha} = 1 \pm \sqrt{1-\left(\eta\frac{\dot{\theta}_{i2}}{p\alpha}\right)^2}. \tag{4.12}$$

The positive sign solution lacks physical meaning because it yields a dimensionless rotation greater than unity. Therefore, the maximum rotation is obtained by the

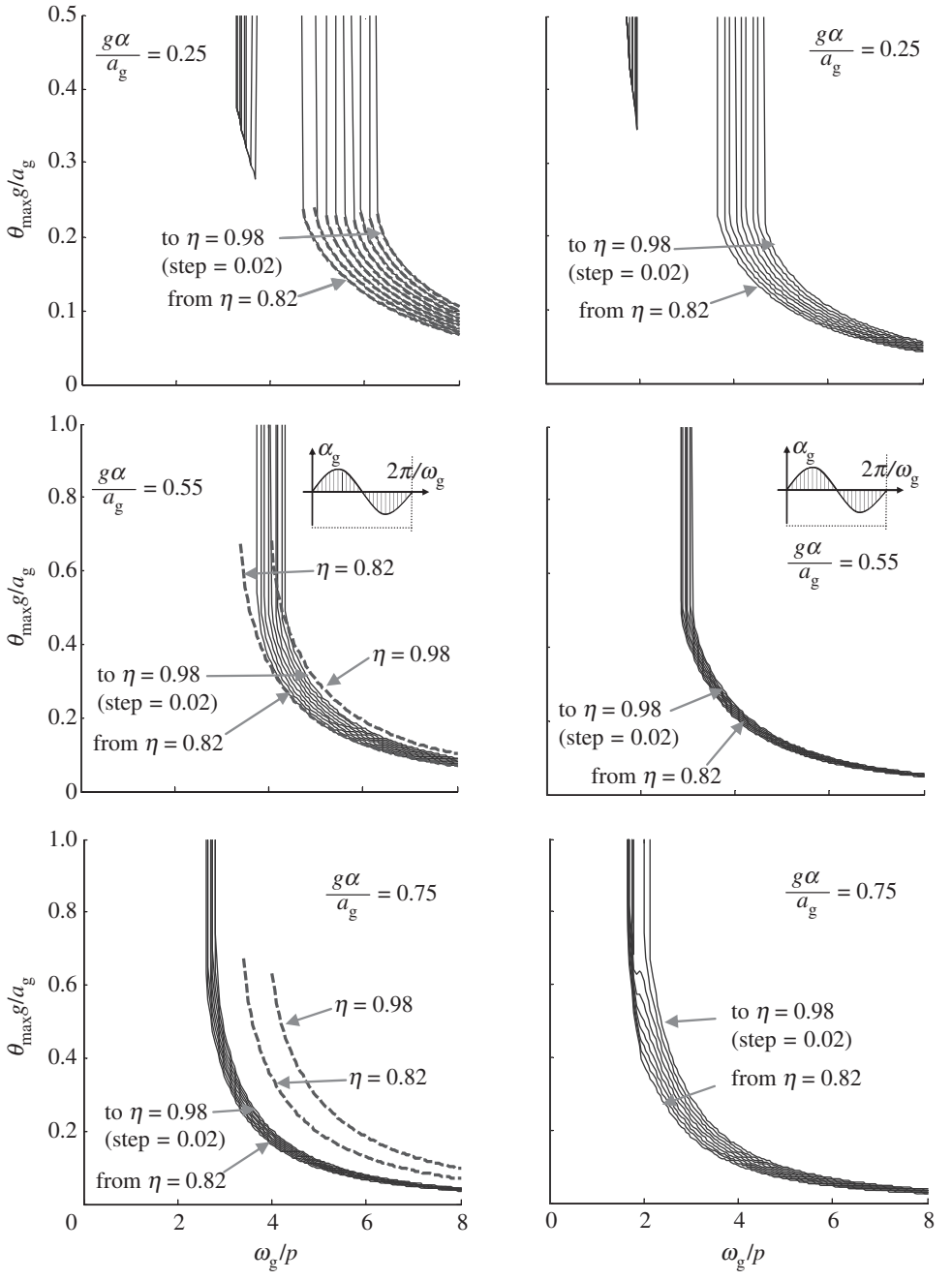

Figure 8. Self-similar rocking spectra for coefficient of restitution values ranging from 0.82 to 0.96 at intervals of 0.02, and different dimensionless slenderness values. Solid lines indicate numerical solutions (equation (3.3)), and dashed lines indicate analytical solutions (equation (4.13)).

negative sign solution as

$$\frac{\theta_m}{\alpha} = 1 - \sqrt{1 - \eta^2(1 - D_0^*)} \quad \text{or} \quad \frac{g\theta_m}{a_g} = \frac{1}{a}\left[1 - \sqrt{1 - \eta^2(1 - D_0^*)}\right], \qquad (4.13)$$

where D_0^* is given by equation (3.9). Equation (4.13) offers a closed-form expression for the rocking spectra and is also plotted in figure 8 (dashed lines). It is accurate when the first impact takes place after the end of the excitation (above the curve $\tau_i = pT_{\rm ex}$; figure 8, top left) and approximate otherwise (below the curve $\tau_i = pT_{\rm ex}$; figure 8, middle left and bottom left). The approximation gets better (figure 8 left) near the curve $\tau_i = pT_{\rm ex}$ that roughly corresponds to $g\alpha/a_g \approx 0.4$ (figure 4). Note that whether the block survives the motion or not can be determined directly with the closed-form expressions. When overturning takes place according to case 1.2, equation (3.18) indicates that $\eta\dot{\theta}_{i2}/p\alpha \geq 1$. Similarly, equation (4.13) yields no real root for $\eta\dot{\theta}_{i2}/p\alpha \geq 1$, also indicating overturning.

The dependence on η in equation (4.13) is complicated, but for small values of $\eta\dot{\theta}_{i2}/p\alpha$ it simplifies to

$$\frac{\theta_{\rm m}}{\alpha} \simeq \frac{\eta^2}{2}\sqrt{1 - D_0^*}, \tag{4.14}$$

or equivalently

$$\frac{g\theta_{\rm m}}{a_g} \simeq \eta^2 \frac{\sqrt{1 - D_0^*}}{2a}. \tag{4.15}$$

Equations (4.14) and (4.15) unveil that the damping effect associated with the coefficient of restitution η (figure 7) results in rocking spectra that can be approximated by a scaling law with respect to η. In particular

$$\frac{\theta_{\rm m}}{\alpha} \simeq \frac{1}{2} f(a, \omega)\eta^2, \tag{4.16}$$

where $f(\alpha, \omega)$ is a function of the two other independent variables (dimensionless slenderness and dimensionless frequency) and is equal to $\sqrt{1 - D_0^*}$ for the case under consideration. Such a similarity law (equation (4.16)) is an example of '*incomplete self-similarity*' (Barenblatt 1996). The applicability of this scaling law should be further investigated in order to derive, if feasible, pertinent closed-form expression for different excitations. However, this analysis is beyond the scope of this paper.

Finally, in the above closed-form expressions (equations (4.13)–(4.16)), the coefficient of restitution η could be replaced with any dependable expression (e.g. equation (2.4)), reducing the arguments of the problem and simplifying further the expression. Under Housner's formulation (equation (2.4)), it is interesting to note that the slenderness α has a twofold effect on rocking which is evident in the proposed dimensionless–orientationless groups. On the one hand, slenderness affects the dimensionless slenderness $1/a = g\tan\alpha/a_{\rm g}$ and on the other hand the damping through the coefficient of restitution η (equation (2.4)).

5. Non-slender block: self-similarity

While the derivations above are satisfactory for many practical engineering applications, the more general case of non-slender blocks, where small-angle assumptions do not hold, should be considered. The associated EOM

(equation (2.2)) can be rewritten as

$$\left.\begin{aligned} &\frac{\ddot{\theta}}{p^2}+\cos\alpha\left[\left(\frac{\ddot{u}_{\mathrm{g}}}{g}\tan\alpha-1\right)\sin\theta+\left(\tan\alpha+\frac{\ddot{u}_{\mathrm{g}}}{g}\right)\cos\theta\right]=0, \quad \theta>0\\ \text{and}\quad &\frac{\ddot{\theta}}{p^2}-\cos\alpha\left[\left(\frac{\ddot{u}_{\mathrm{g}}}{g}\tan\alpha+1\right)\sin\theta+\left(\frac{\ddot{u}_{\mathrm{g}}}{g}-\tan\alpha\right)\cos\theta\right]=0, \quad \theta<0. \end{aligned}\right\} \tag{5.1}$$

Because the notions of dimension and orientation are differentiated, the dimensionless–orientationless groups of equations (4.10) and (4.11) are only valid for small values of α (slender blocks) for which the linearized EOM hold true. For non-slender blocks (and large rotations), the orientations of the governing parameters are slightly different. Instead of equation (4.3), the response function, taking into account the orientations of the involved parameters (see equations (4.6) and (4.7)), can be written as

$$\theta_{\max}=\phi\left(\frac{\omega_{\mathrm{g}}}{p},\frac{a_{\mathrm{g}}}{g},\tan\alpha,\cos\alpha,\eta\right). \tag{5.2}$$

The dimensionless–orientationless groups become

$$\frac{\theta_{\max}g}{a_{\mathrm{g}}}=\phi\left(\frac{\omega_{\mathrm{g}}}{p},\frac{g\tan\alpha}{a_{\mathrm{g}}},\cos\alpha,\eta\right). \tag{5.3}$$

The dimensionless slenderness $(g\tan\alpha)/a_{\mathrm{g}}$ is exactly the expression that determines the base acceleration for which a non-slender block enters the rocking motion. Strictly speaking, this is as far as dimensional–orientational analysis can take us, because all of the terms in equation (5.3) are orientationless, including $\theta_{\max}g/a_{\mathrm{g}}$ and $\cos\alpha$. Contrary to the case of slender blocks and small rotations, the slenderness angle cannot be incorporated entirely into the other dimensionless–orientationless arguments because it also appears as an isolated parameter $\cos\alpha$. Practically, this means that non-slender blocks can exhibit a self-similar rocking response only if they are geometrically similar (same slenderness). The overturning plots in figure 9 illustrate the self-similar response of two (non-slender) geometrically similar blocks ($\alpha=20^\circ$) of different size ($R=0.5\,\mathrm{m}$ and $1.0\,\mathrm{m}$). The overturning plots collapse to a single curve for a given excitation (figure 9).

The explicit dependence of the response of non-slender blocks on α is demonstrated by the overturning plots in figure 10. Note that the dependence is relatively small for $\alpha<15^\circ$, and that as α decreases, the sine impulse curves converge towards the relevant closed-form solution for slender blocks (figure 4). This convergence is expected, as the dimensionless–orientationless terms of equation (5.3) collapse to those of equation (4.11) for slender blocks. For large non-slender blocks that undergo large rotations, further simplification is not possible. However, figure 10 indicates that when the rocking rotation remains small, the dependence on the slenderness angle α is explicit but it is consistent and weak (figure 11).

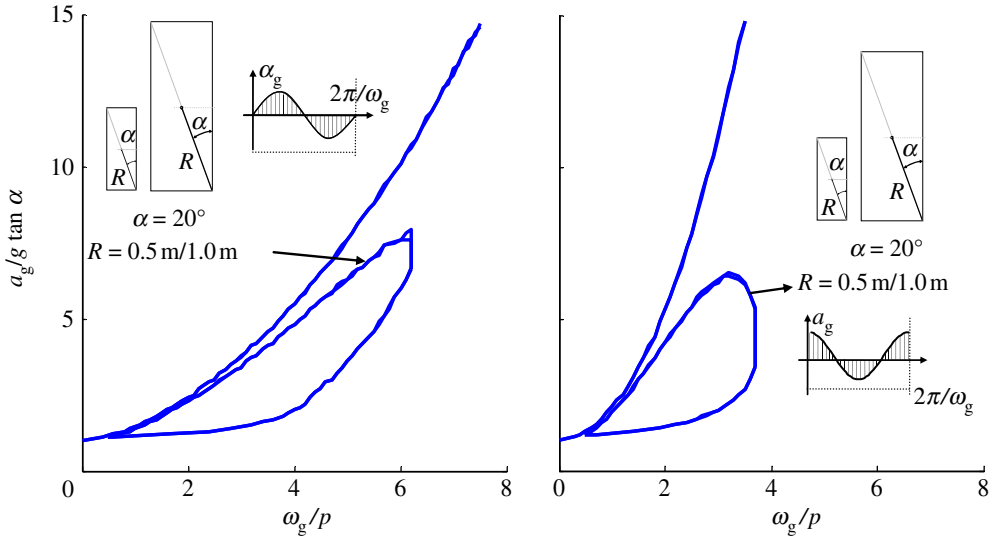

Figure 9. Self-similar overturning plots for geometrically similar non-slender blocks of different scale ($\eta = 0.85$). (Online version in colour.)

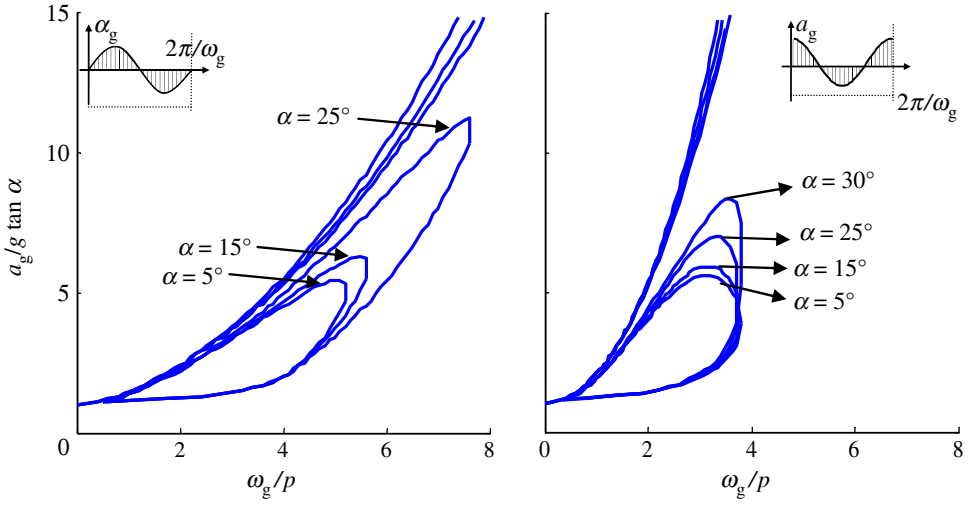

Figure 10. Self-similar overturning plots for non-slender blocks with different slenderness angle α ($\eta = 0.85$). (Online version in colour.)

6. Non-slender block small rotations: approximate self-similarity

Owing to the weak dependence on α for small rotation angles, the rocking response of non-slender blocks with small rotations is considered separately. In this case, it is practically useful to eliminate $\cos\alpha$ as an independent group, resulting in equation (6.1)

$$\frac{\theta g}{a_g \cos\,\alpha} \simeq \phi\left(\frac{\omega_g}{p}, \frac{g\tan\alpha}{a_g}, \eta\right). \tag{6.1}$$

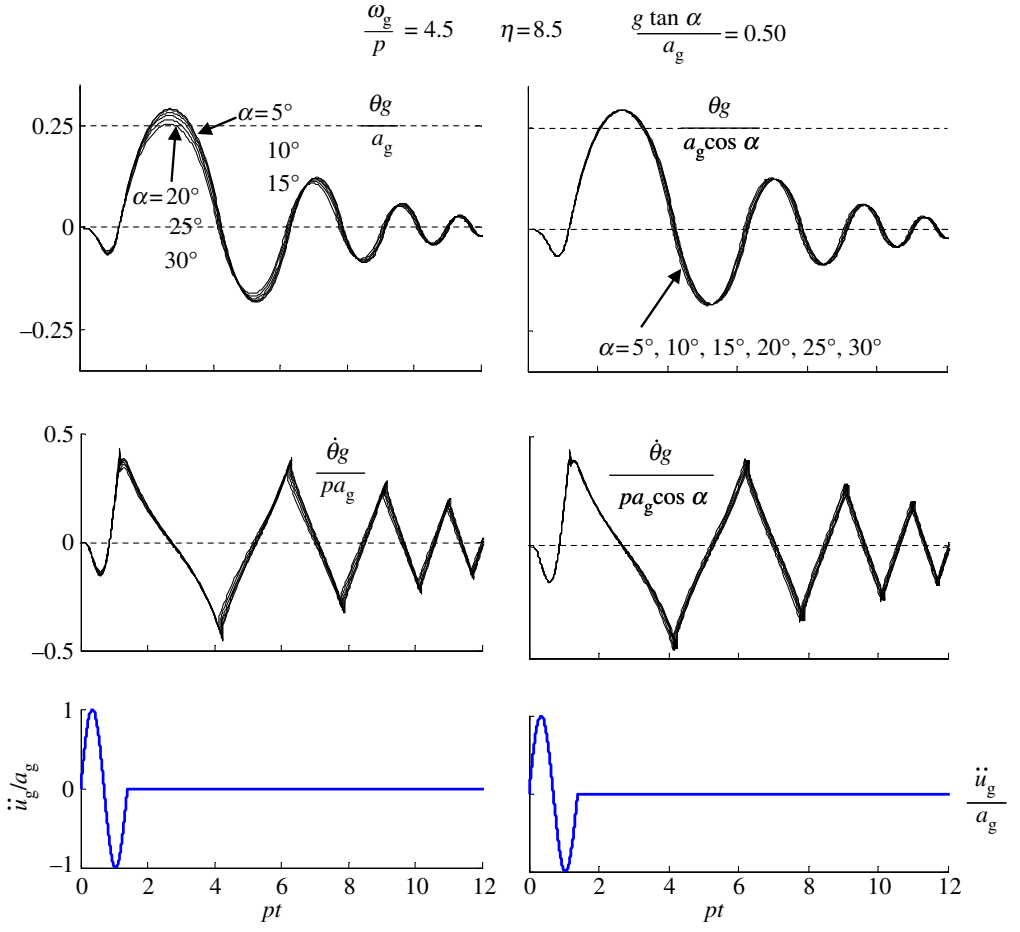

Figure 11. Rocking response: non-self-similar response (left), and self-similar response (right). (Online version in colour.)

This formulation is not perfectly self-similar but it is practically (approximately) self-similar for $g\tan\alpha/a_g$ near unity, say $0.5 < g\tan\alpha/a_g < 1$. This is demonstrated in figure 11, where the rocking responses of non-slender blocks with different geometry are calculated using the nonlinear EOM (equation (2.2)). Results are presented in the proposed dimensionless–orientationless groups derived for small angles (left) and for large angles (right). The right column shows notably less dependence on α. Larger α values than presented in figure 11 need not be considered because the fundamental assumption of pure rocking behaviour (without sliding or bouncing) would likely break down.

In figure 12, the necessity to use the practically self-similar description (equation (6.1)) for a larger value of dimensionless slenderness ($g\tan\alpha/a_g = 0.75$) is investigated. In this case, it is even more evident that the response is (approximately) self-similar only if the appropriate groups (equation (6.1)) are adopted.

Extending the same concept, rocking response spectra are plotted in the proposed dimensionless–orientationless terms in figure 13 are also practically

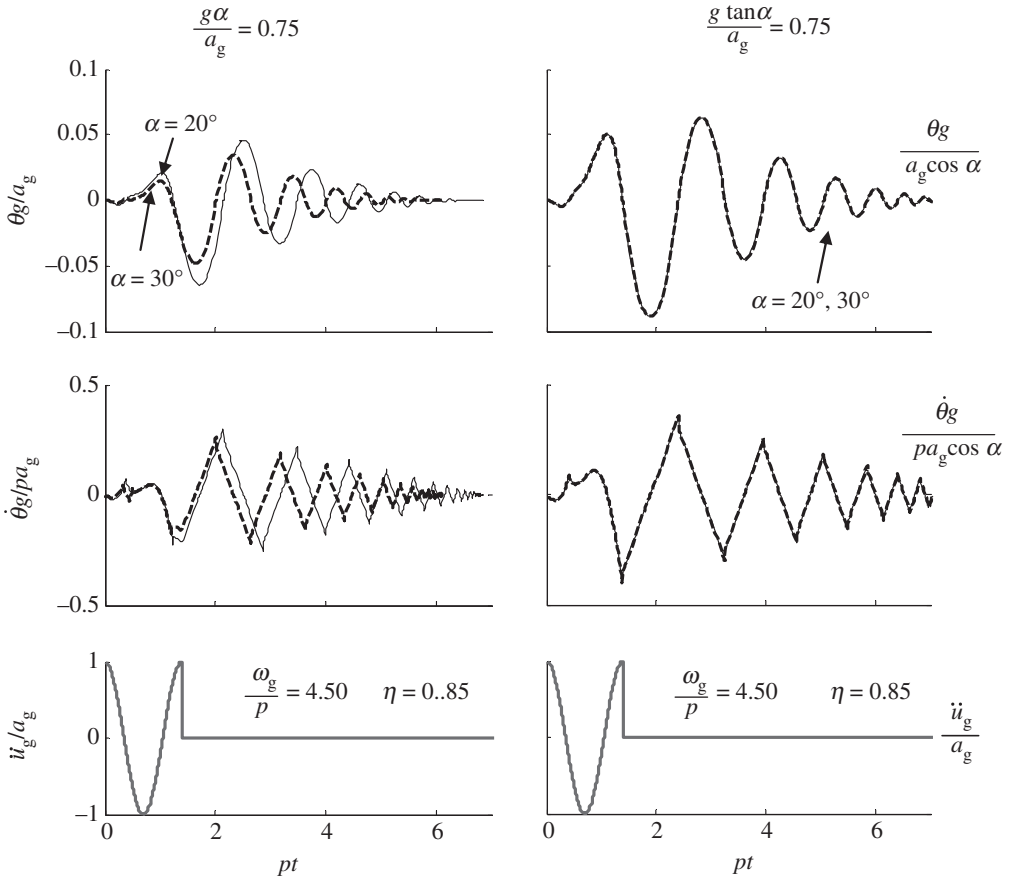

Figure 12. Nonlinear response for the proposed dimensionless–orientationless groups derived for small angles (equation (4.1), left column, not self-similar) and for large angles (equation (6.1), right column, practically self-similar).

self-similar and indifferent to the intensity and the frequency content of the excitation (figure 13). Note that similar overturning plots were presented in figure 10 for the slender block formulation. In most cases, the overturning contours for different slenderness values collapse to a single curve, confirming practical self-similarity and therefore indifference to the intensity and the frequency content of the excitation. It is again evident that the proposed groups (equation (6.1)) are most effective for larger values of dimensionless slenderness ($g \tan\alpha/a_g$). On the basis of these results, the use of the dimensionless–orientationless groups for large rotations (equation (6.1)) is proposed for all cases (both slender and non-slender blocks), because they are nearly exact for small rotations and an effective approximation for small rotations of non-slender blocks.

7. Conclusions

In this paper, the response of the stand-alone rocking block under a simple pulse excitation is revisited. Closed-form solutions that define completely

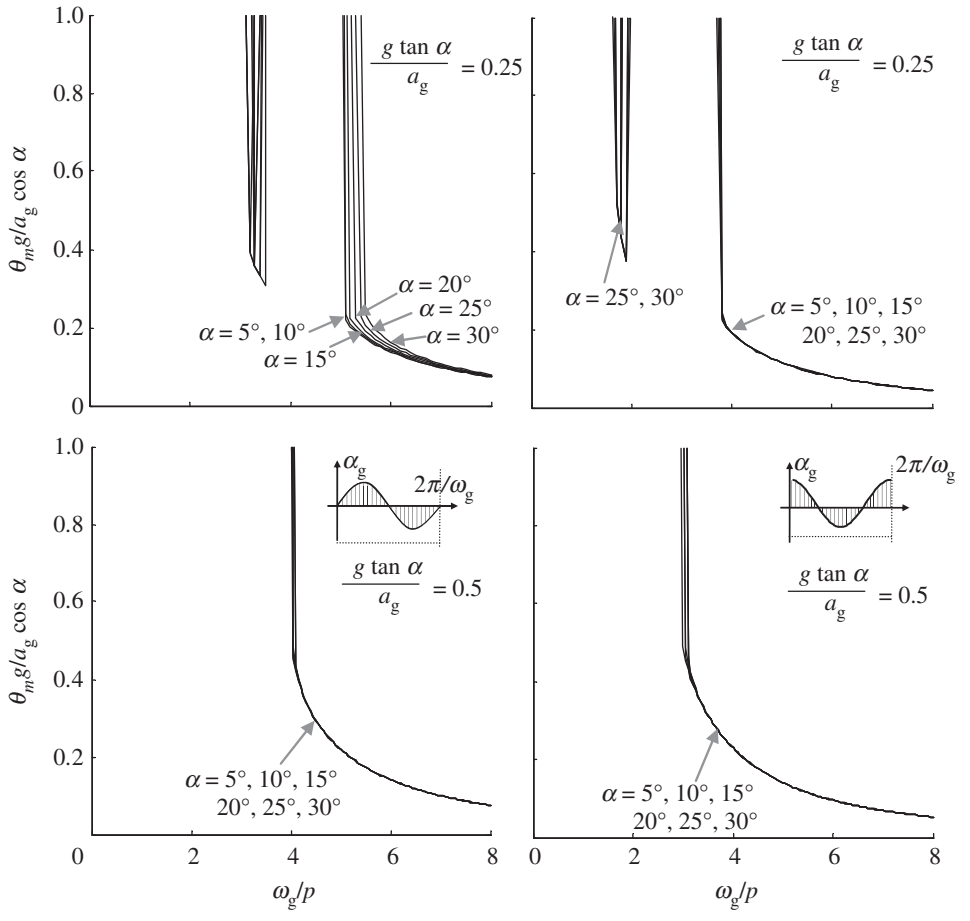

Figure 13. Rocking spectra presented using the dimensionless–orientationless groups derived for non-slender blocks (equation (6.1)) for a given coefficient of restitution ($\eta = 0.85$) but different slenderness.

the overturning areas of the linearized rocking block, on the control space, are derived. These expressions are achieved after solving the associated transcendental equations to calculate the time of impact, either exactly or approximately, through an original procedure. To this end, a novel ad hoc method for approximating the involved transcendental equation is proposed. This formulation is practically useful, as it provides a quick method for directly plotting overturning curves without extensive repeated numerical simulation and provides insight into the mechanism behind the overturning of the rocking block.

In this context, it is shown that standard dimensional analysis does not yield a useful scaling of the rocking problem. To tackle this challenge, the proposed approach builds upon the closed-form solution and hinges upon the differentiation of the notions of dimension and orientation. The dimensionless–orientationless products derived condense the description of the rocking problem and unveil the symmetry of self-similarity even though the response is nonlinear and

non-smooth. Critically, the coefficient of restitution is treated as an independent parameter of the rocking behaviour, to which the derived closed-form scaling relation can be applied, allowing a single two-dimensional response spectrum to completely describe the maximum rocking response of any slender block. Finally, the study proposes a set of dimensionless–orientationless parameters for non-slender blocks. These parameters allow a description of the response that is exactly self-similar for small rotations, and practically self-similar for large rotations. In summary, new methods for generating general overturning plots and response spectra, for both slender and non-slender blocks of any geometry, are provided.

The first author gratefully acknowledges the contribution of Prof. Nicos Makris in motivating some of the ideas presented herein. Financial support for this research was provided by the Engineering and Physical Sciences Research Council of the United Kingdom under grant reference number EP/H032657/1.

Appendix A. Exact solution of equation (3.12)

Equation (3.12) is a transcendental equation of the form

$$I_1 e^{-\tau} + I_2 e^{\tau} + I_3 = 0 \tag{A 1}$$

which can be rewritten as

$$e^{-\tau}(I_1 + I_2 e^{2\tau} + I_3 e^{\tau}) = 0, \tag{A 2}$$

where I_1, I_2 and I_3 are (independent of time τ) constants. Introducing the change of variable $x = e^{\tau}$, equation (A 1) becomes

$$\frac{1}{x}(I_2 x^2 + I_3 x + I_1) = 0. \tag{A 3}$$

Equation (A 3), for positive x, yields a simple quadratic equation

$$I_2 x^2 + I_3 x + I_1 = 0. \tag{A 4}$$

References

Anooshehpoor, A., Heaton, T. H., Shi, B. & Brune, J. N. 1999 Estimates of the ground accelerations at point Reyes station during the 1906 San Francisco earthquake. *Bull. Seismol. Soc. Am.* **89**, 845–853.

Araneda, J. 1996 Dimensional-directional analysis by a quaternionic representation of physical quantities. *J. Franklin Inst.* **333**, 113–126. (doi:10.1016/0016-0032(96)85843-1)

Augusti, G. & Sinopoli, A. 1992 Modelling the dynamics of large block structures. *Meccanica* **27**, 195–211. (doi:10.1007/BF00430045)

Barenblatt, G. 1996 *Scaling, self-similarity, and intermediate asymptotics*. Cambridge, UK: Cambridge University Press.

Brogliato, B. 1999 *Nonsmooth mechanics: models, dynamics, and control*, 2nd edn. London, UK: Springer.

Buckingham, E. 1914 On physically similar systems; illustrations of the use of dimensional equations. *Phys. Rev.* **4**, 345–376. (doi:10.1103/PhysRev.4.345)

Contento, A. & Di Egidio, A. 2009 Investigations into the benefits of base isolation for non-symmetric rigid blocks. *Earthq. Eng. Struct. Dyn.* **38**, 849–866. (doi:10.1002/eqe.870)

DeJong, M. J. In press. Amplification of rocking due to horizontal ground motion. *Earthq. Spectra*.

DeJong, M. J., De Lorenzis, L., Adams, S. & Ochsendorf, J. A. 2008 Rocking stability of masonry arches in seismic regions. *Earthq. Spectra* **24**, 847–865. (doi:10.1193/1.2985763)

Dimitrakopoulos, E. G. & DeJong, M. J. In press. Overturning of retrofitted rocking structures under pulse-type excitation. *J. Eng. Mech.* (*ASCE*) (doi:10.1061/(ASCE)EM.1943-7889.0000410).

Dimitrakopoulos, E. G., Kappos, A. J. & Makris, N. 2009*a* Dimensional analysis of yielding and pounding structures for records without distinct pulses. *Soil Dyn. Earthq. Eng.* **29**, 1170–1180. (doi:10.1016/j.soildyn.2009.02.006)

Dimitrakopoulos, E. G., Makris, N. & Kappos, A. J. 2009*b* Dimensional analysis of the earthquake-induced pounding between adjacent structures. *Earthq. Eng. Struct. Dyn.* **38**, 867–886. (doi:10.1002/eqe.872)

Dimitrakopoulos, E. G., Makris, N. & Kappos, A. J. 2010 Dimensional analysis of the earthquake-induced pounding between inelastic structures. *Bull. Earthq. Eng.* **9**, 561–579. (doi:10.1007/s10518-010-9220-8)

ElGawady, M. A., Ma, Q., Butterworth, J. W. & Ingham, J. 2010 Effects of interface material on the performance of free rocking blocks. *Earthq. Eng. Struct. Dyn.* **40**, 375–392. (doi:10.1002/eqe.1025)

Glocker, C. 2001 On frictionless impact models in rigid-body systems. *Phil. Trans. R. Soc Lond. A* **359**, 2385–2404. (doi:10.1098/rsta.2001.0857)

Hogan, S. J. 1989 On the dynamics of rigid-block motion under harmonic forcing. *Proc. R. Soc. Lond. A* **425**, 441–476. (doi:10.1098/rspa.1989.0114)

Hogan, S. J. 1990 The many steady state responses of a rigid block under harmonic forcing. *Earthq. Eng. Struct. Dyn.* **19**, 1057–1071. (doi:10.1002/eqe.4290190709)

Housner, G. W. 1963 The behavior of inverted pendulum structures during earthquakes (in an engineering report on the Chilean earthquakes on May 1960, Housner). *Bull. Seismol. Soc. Am.* **53**, 403–417.

Makris, N. & Black, C. J. 2004 Dimensional analysis of rigid-plastic and elastoplastic structures under pulse-type excitations. *J. Eng. Mech.* **130**, 1006–1018. (doi:10.1061/(ASCE)0733-9399(2004)130:9(1006))

Makris, N. & Psychogios, T. 2006 Dimensional response analysis of yielding structures with first-mode dominated response. *Earthq. Eng. Struct. Dyn.* **35**, 1203–1224. (doi:10.1002/eqe.578)

Mylonakis, G. & Voyagaki, E. 2006 Yielding oscillator subjected to simple pulse waveforms: numerical analysis & closed-form solutions. *Earthq. Eng. Struct. Dyn.* **35**, 1949–1974. (doi:10.1002/eqe.615)

Priestley, M. J. N., Evison, R. J. & Carr, A. J. 1978 Seismic response of structures free to rock on their foundations. *Bull. N.Z. Natl. Soc. Earthq. Eng.* **11**, 1978–1909.

Prieto, F., Lourenço, P. B. & Oliveira, C. S. 2004 Impulsive Dirac-delta forces in the rocking motion. *Earthq. Eng. Struct. Dyn.* **33**, 839–857. (doi:10.1002/eqe.381)

Sedov, L. 1992 *Similarity and dimensional methods in mechanics*, 10th edn. Boca Raton, FL: CRC Press.

Siano, D. 1985 Orientational analysis: a supplement to dimensional analysis: I. *J. Franklin Inst.* **320**, 267–283. (doi:10.1016/0016-0032(85)90031-6)

Yilmaz, C., Gharib, M. & Hurmuzlu, Y. 2009 Solving frictionless rocking block problem with multiple impacts. *Proc. R. Soc. A* **465**, 3323–3339. (doi:10.1098/rspa.2009.0273)

Zhang, J. & Makris, N. 2001 Rocking response of free-standing blocks under cycloidal pulses. *J. Eng. Mech.* **127**, 473. (doi:10.1061/(ASCE)0733-9399(2001)127:5(473))